EBioMedicine 47 (2019) 195–207

Contents lists available at ScienceDirect

EBioMedicine

journal homepage: www.ebiomedicine.com

EBioMedicine
Published by THE LANCET

Research paper

N^6-methyladenosine modification of ITGA6 mRNA promotes the development and progression of bladder cancer

Huan Jin [a,b,1], Xiaoling Ying [a,1], Biao Que [c], Xiaoxue Wang [d], Yinghui Chao [a], Haiqing Zhang [a], Zusen Yuan [c], Defeng Qi [c], Shuibin Lin [a], Wang Min [e], Mei Yang [f,**], Weidong Ji [a,*]

[a] Center for Translational Medicine, The First Affiliated Hospital, Sun Yat-sen University, 510080 Guangzhou, China
[b] Department of Physiology, Zunyi Medical College, Guizhou 563000, China
[c] Department of Urology, Minimally Invasive Surgery Center, The First Affiliated Hospital of Guangzhou Medical University, Guangdong Key Laboratory of Urology, Guangzhou 510230, China
[d] Department of Colorectal Surgery, The Sixth Affiliated Hospital of Sun Yat-sen University, Guangzhou 510655, China
[e] Department of Pathology and the Vascular Biology and Therapeutics Program, Yale University School of Medicine, New Haven, CT 06519, USA
[f] Department of Breast Surgery, Guangdong Provincial People's Hospital, Guangzhou 510080, China

ARTICLE INFO

Article history:
Received 1 April 2019
Received in revised form 21 July 2019
Accepted 29 July 2019
Available online 10 August 2019

Keywords:
N^6-methyladenosine
ITGA6
METTL3
Progression
Bladder cancer

ABSTRACT

Background: Accumulating evidence has revealed the critical roles of N^6-methyladenosine (m^6A) modification of mRNA in various cancers. However, the biological function and regulation of m^6A in bladder cancer (BC) are not yet fully understood.
Methods: We performed cell phenotype analysis and established *in vivo* mouse xenograft models to assess the effects of m^6A-modified ITGA6 on BC growth and progression. Methylated RNA immunoprecipitation (MeRIP), RNA immunoprecipitation and luciferase reporter and mutagenesis assays were used to define the mechanism of m^6A-modified ITGA6. Immunohistochemical analysis was performed to assess the correlation between METTL3 and ITGA6 expression in bladder cancer patients.
Findings: We show that the m^6A writer METTL3 and eraser ALKBH5 altered cell adhesion by regulating ITGA6 expression in bladder cancer cells. Moreover, upregulation of ITGA6 is correlated with the increase in METTL3 expression in human BC tissues, and higher expression of ITGA6 in patients indicates a lower survival rate. Mechanistically, m^6A is highly enriched within the ITGA6 transcripts, and increased m^6A methylations of the ITGA6 mRNA 3'UTR promotes the translation of ITGA6 mRNA *via* binding of the m^6A readers YTHDF1 and YTHDF3. Inhibition of ITGA6 results in decreased growth and progression of bladder cancer cells *in vitro* and *in vivo*. Furthermore, overexpression of ITGA6 in METTL3-depleted cells partially restores the BC adhesion, migration and invasion phenotypes.
Interpretation: Our results demonstrate an oncogenic role of m^6A-modified ITGA6 and show its regulatory mechanisms in BC development and progression, thus identifying a potential therapeutic target for BC.
Fund: This work was supported by National Natural Science Foundation of China (81772699, 81472999).

1. Introduction

Bladder cancer (BC) is one of the most common urogenital cancers, with an estimated 549,000 new cases and 200,000 deaths in 2018 [1]. BC is classified as non- muscle-invasive BC (NMIBC) and muscle-invasive BC (MIBC). NMIBCs, which account for approximately 75% of BC, frequently recur, and in 10–30% of patients, NMIBC progresses to MIBC, which has a reduced survival rate and frequent distant metastasis [2]. Despite recent advances in pathological diagnosis and clinical treatment, BC remains a major cause of cancer-related morbidity and mortality due to high heterogeneity and recurrence rates together with limited treatment options [3,4]. Therefore, there is an urgent need to characterize the underlying molecular mechanism of BC tumorigenesis for the development of new therapeutic strategies.

Dynamic epigenetic modification of DNA and histone plays a critical role in gene expression. In recent years, RNA modifications, collectively referred to as the "epitranscriptomes", have been suggested to represent an additional layer of gene regulation [5]. Among these

* Correspondence to: W. Ji, Center for Translational Medicine, The First Affiliated Hospital, Sun Yat-sen University, Guangzhou, Guangdong 510080, China.
** Correspondence to: M. Yang, Department of Breast Cancer, Cancer Center, Guangdong Provincial People's Hospital, Guangdong Academy of Medical Sciences, Guangzhou, Guangdong 510080, China.
E-mail addresses: bayberry513@yahoo.com (M. Yang), jiweidong@mail.sysu.edu.cn (W. Ji).
[1] Contributed equally to the manuscript.

https://doi.org/10.1016/j.ebiom.2019.07.068

Research in context

Evidence before this study

Emerging studies have revealed that m^{6}A modification and the associated regulatory proteins play critical roles in the pathogenesis of various types of cancers. However, the expression pattern of the same m^{6}A-regulated proteins and their target mRNAs may differ in various cancers, indicating that the m^{6}A modification pathway could have oncogenic or tumour-suppressive functions in different types of tumours. Recently, our study and another study showed that METTL3 promotes bladder cancer progression. Because thousands of genes exhibit m^{6}A modification, the mechanistic link between m^{6}A and BC development warrants further investigation. ITGA6 has been shown to play an important role in the development and progression of various types of cancers. Although the expression levels of ITGA6 were significantly associated with the incidence of intravesical recurrence and ITGA6 is one of 18 genes that defined the "tumour differentiation signature" applied for BC stratification, its role in BC is largely unknown.

Added value of this study

We provide evidence that the m^{6}A writer METTL3 and eraser ALKBH5 modulate ITGA6 expression through m^{6}A-based post-transcriptional regulation; the m^{6}A readers YTHDF1/YTHDF3 preferentially recognize m^{6}A residues in the ITGA6 3′UTR, and promote the ITGA6 translation, revealing a novel regulatory pathway of m^{6}A-modified ITGA6 in BC. Importantly, we demonstrate that ITGA6 is a critical downstream target of METTL3 in promoting the growth and progression of bladder cancer cells *in vitro* and *in vivo*. These findings not only uncover an oncogenic role of ITGA6 in BC development and progression, but also reveal a novel post-transcriptional, m^{6}A-dependent mechanism of ITGA6 expression.

Implications of all the available evidence

Our study provides a promising therapeutic target for the treatment of BC by revealing the oncogenic role of m^{6}A-modified ITGA6 and its regulatory mechanisms in BC development and progression.

modifications, N6-methyladenosine (m^{6}A) modification is the most abundant internal modification of mRNAs. m^{6}A modification is catalysed by the m^{6}A methyltransferase complex ("writer") composed of Methyltransferase-like 3 and 14 (METTL3 and METTL14), Wilms tumour 1-associated protein (WTAP), vir like m^{6}A methyltransferase associated (VIRMA, also known as KIAA1429), RNA-binding motif protein 15 (RBM15) and zinc finger CCCH-type containing 13 (ZC3H13) [6–9], and can be removed by m^{6}A demethylases ("erasers") including FTO and ALKBH5 [10,11]. A group of YT521-B homology (YTH) domain-containing proteins (YTHDFs) have been identified as m^{6}A readers that can recognize m^{6}A marks and mediate m^{6}A functions [12–14]. Recent studies have shown that m^{6}A modification can regulate multiple RNA-related processes, such as RNA stability [13], translation [14], and alternative splicing [15,16]. Emerging studies have revealed that m^{6}A modification and the associated regulatory proteins play critical roles in the pathogenesis of various types of cancers [17–23], including leukaemia, brain tumour, breast cancer, liver cancer, cervical cancer, endometrial cancer, and lung cancer. Moreover, numerous target genes modified by m^{6}A play essential regulatory roles in tumour occurrence and development [19,24]. However, the expression pattern of these m^{6}A-regulated proteins and their target mRNAs may differ in various cancers, indicating that the m^{6}A modification pathway could play an oncogenic or tumour-suppressive role in different types of tumours [24,25]. To date, knowledge of the mechanistic link between m^{6}A and BC development is rather limited.

In our previous studies, we found that METTL3 expression is upregulated in human bladder cancer samples and associated with bladder cancer progression. Additionally, METTL3 promotes the bladder cancer tumorigenesis [26]. To further investigate the functions and the underlying molecular mechanisms of m^{6}A modification and the associated regulatory targets in BC development, we identified adhesive molecule integrin alpha-6 (ITGA6) as a target of m^{6}A modification regulated by METTL3 and ALKBH5. ITGA6 is a member of the Integrin family that is known to mediate interactions with the ECM and enhance multiple cell motility and cell signalling outputs. ITGA6 is overexpressed in multiple types of cancers, promoting tumorigenesis and metastasis [27–29]. However, the role and underlying molecular mechanisms of ITGA6 in bladder cancer are unclear. Our results reveal an oncogenic role of m^{6}A-modified ITGA6 and its regulatory mechanisms in BC development and progression, identifying a potential therapeutic target for BC.

2. Materials and methods

2.1. Clinical samples

FFPE tissues from 186 bladder cancer patients in this study, who underwent radical cystectomy and bladder biopsies between February 2010 and September 2017, were obtained from the the Department of Pathology archives at the First Affiliated Hospital of Sun Yat-sen University (Guangzhou, China) and the First Affiliated Hospital of Guangzhou Medical University (Guangzhou, China). A bladder cancer tissue microarray (HBlaU066Su01) was purchased from Shanghai Outdo Biotech. This study was approved by the Institutional Ethics Committee for Clinical Research and Animal Trials of the First Affiliated Hospital of Sun Yat-sen University [(2016)067]. Informed consent was obtained from all patients prior to analysis.

2.2. Immunohistochemistry

Paraffin sections with a thickness of 4 μm were baked for 2 h at 55 °C. Prior to immunostaining, paraffin sections were deparaffinized and rehydrated in an alcohol series, followed by antigen retrieval with microwave (MW) heating in Tris-EDTA buffer (pH 9.0). Sections were blocked with 5% normal goat serum and incubated with the appropriate primary antibodies (anti-METTL3, CST, 1:100 dilution; anti-ITGA6, CST, 1:100 dilution) at 4 °C overnight. Then immunoreactions were detected with an UltraSensitive™ S-P Ultrasensitive Kit (HRP, anti-rabbit) and visualized with DAB substrate. Images were acquired with a ZEISS Axio Imager.Z2 Microscope. IHC staining was assessed using a semi-quantitative scoring method by recording both the area of positive staining and the staining intensity. The area of positive staining was defined as 0%, <25%, 25%–50%, 50%–75% or >75% positively stained cells and was scored as 1, 2, 3, or 4, respectively. The staining intensity was defined as no staining (0), weak staining (1), moderate staining (2), or strong staining (3). The immunoreactivity score (IHS) was calculated by multiplying the positive area scores by the staining intensity score. An IHS of <8 was defined as low expression, and an HIS of ≥8 was defined as high expression.

2.3. Cell culture

Human uroepithelial cells (SV-HUC-1) and 293T cells were obtained from the American Type Culture Collection (Manassas, VA). The human bladder cancer cell lines T24, UM-UC-3, 5637, and J82 were purchased from the Institute of Cell Biology, Chinese Academy of Sciences (Shanghai, China). SV-HUC-1 or 293T cells with overexpression of METTL3

(OE-METTL3) or depletion of ALKBH5 (KO-ALKBH5), T24 or UM-UC-3 cells overexpression of ALKBH5 (OE-ALKBH5) or depletion of METTL3 (KO-METTL3) were generated in our laboratory. SV-HUC-1 cells were cultured in Ham's F-12K (Kaighn's) medium (Gibco, USA), and 293T cells were cultured in DMEM (Gibco, USA). T24 cells and 5637 cells were cultured in RPMI1640 medium (Gibco, USA), and UM-UC-3 cells and J82 cells were cultured in MEM (Gibco, USA). All media were supplemented with 10% foetal bovine serum (Gibco, USA). Cells were cultured in a water-saturated atmosphere under 5% CO_2 at 37 °C. All cell lines tested negative for mycoplasma contamination using a PCR-based universal mycoplasma detection kit.

2.4. Plasmid construction and mutagenesis assays

ITGA6 expression plasmids were generated by cloning the full-length ORF of human ITGA6 (NM_ 001079818.2) into the LentiORF PLEX vector. Lentivira vectors expressing sgRNA targeting ITGA6 were constructed according to the lentiCRISPR v2 protocol. The lentiCRISPR v2 plasmid was a gift from Feng Zhang (Addgeneplasmid#52961).The sgRNAs with the highest scores and least off-target effects were selected using an online tool (https://chopchop.rc.fas.harvard.edu/index.php). The sgRNAs sequences are listed in Table S1. The 3′UTR of ITGA6 was cloned from HUVECs. ITGA6–3′UTR was inserted into the dual-luciferase-containing psiCHECK™-2 vector (Promega). The DNA fragments of the psiCHECK™-2-ITGA6 3'UTR containing the wild-type m^6A motifs as well as the mutant motifs (in which A was replaced by T) were generated by site-directed mutagenesis. The primers used for mutagenesis are listed in Table S1.

2.5. Lentiviral transduction to establish stable cell lines

For virus transduction, 293T cells were transfected with the appropriate lentiviral vector according to the Lipofectamine® 3000 reagent (Invitrogen) protocol. The LentiORF pLEX-MCS vector was used for overexpression, with the target plasmid and the packaging plasmids pCMV-dR8.2-dvpr and PLP-VSVG at a 1:1:0.5 ratio. The LentiCRISPR v2 was used for CRISPR-Cas9, with the target plasmid and the packaging plasmids PAX2 and PLP-VSVG at a 1:1:0.5 ratio. To establish stable cell lines, target cells were transduced by using the above lentiviruses with polybrene (8 μg /ml, Sigma). After 12 h of transduction, cells were cultured further. Then the cells were selected with 1 μg /ml puromycin (Sigma) for 5 days.

2.6. RNA isolation and qRT-PCR

Total RNA was extracted using TRIzol (Invitrogen) according to the manufacturer's instructions. cDNA synthesis was performed using PrimeScript™RT Reagent Kit with gDNA Eraser (TaKaRa). Quantitative real-time PCR (qPCR) using Fast SYBR Green PCR Master Mix (Applied Biosystems) was performed on a Step-One Fast Real-time PCR System (Applied Biosystems). All data were analysed using the $2^{-\triangle\triangle CT}$ method. The primer sequences are shown in Table S1.

2.7. Western blotting analysis

SDS loading buffer was added to samples and boiled for 10 min. Samples were loaded on 8–10% SDS-PAGE gels and subjected to immunoblotting with different antibodies (see Table S2). After incubation with horseradish-peroxidase-conjugated secondary antibodies (CST) at room temperature for 1 h, immunorections were visualized using ECL Plus (Thermo Scientific). The band intensities were measured by ImageJ.

2.8. Cell adhesion assay

Briefly, cells were seeded in equal numbers into 96-well plates previously coated with laminin (12 μg/ml, Corning). Cells were incubated in a CO_2 incubator at 37 °C for 1 h. Then, cells were fixed with 4% paraformaldehyde for 15 min and stained with crystal violet for 10 min. Images were acquired with a ZEISS Axio Imager.Z2 microscope. Plates were incubated with 2% SDS at room temperature for 30 min and read at 570 μm.

2.9. Cell proliferation assay

A total of 5000 cells were seeded into each well of five 96-well culture plates and cultured in a humidified, 5% CO_2 atmosphere. One 96-well plate was removed at 24 h, 48 h, 72 h, 96 h, and 120 h, and add 20 μl of CellTiter 96® AQueous One Solution Reagent (Promega) in 100 μl of culture medium was added to each well containing samples. The plate was incubated the plate at 37 °C for 2 h in a humidified, 5% CO_2 atmosphere. Finally, the absorbance was recorded at at 490 nm using a SYNERGY H1 microplate reader (Bio Tek).

2.10. Cell migration assay

A total of 1×10^5 cells were plated in 96-well Image-Lock plates (Essen Bioscience). Cells were examined for confluency as a monolayer *via* light microscopy before scratch wounds were made. Scratches were made by using a Wound Maker™ (Essen BioScience). The medium was replaced with medium containing 1% foetal bovine serum (FBS). Plate were placed into the IncuCyte ZOOM™ (Essen BioScience) apparatus, and images of the collective cell spreading were recorded every 1 h for a total duration of 24 h.

2.11. Cell invasion assay

Transwell Matrigel invasion assays were performed using 24-well Transwell inserts with an 8 μm pore size (Corning). First, a 24-well permeable support plate was coated with 200–300 μg/ml of Corning Matrigel matrix (Corning Cat. No. 354234). After 24 h, 1×10^5 cells in 200 μl of culture medium without FBS were plated in the upper chambers, and 500 μl of culture medium containing 20% FBS was placed in each bottom chamber and incubated for 24 h at 37 °C. The invaded cells were fixed with 100% methanol for 30 min and stained with 0.1% crystal violet solution for 30 min at room temperature. The invaded cells were counted under a ZEISS Axio Imager.Z2 microscope.

2.12. Flow cytometry

After cell digestion, cells were washed with PBS, and primary antibody (integrin α6/CD49f, 2.5 μg/10^6 cells, R&D Systems) was added for 30 min in a dark chamber. Cells were detected by flow cytometry (Beckman Coulter) and data were analysed using Summit v. 5.3.

2.13. Methylated RNA immunoprecipitation (MeRIP)

The MeRIP assay was performed according to the reported protocol [30]. Briefly, anti-m^6A primary antibody (Synaptic Systems) was incubated with Pierce™ Protein A/G Magnetic Beads (Thermo Scientific) for 3 h at 4 °C. Then, mRNA was fragmented with an RNA fragmentation kit (Ambion) and incubated with the mixture overnight at 4 °C. Captured RNA was washed 5 times, eluted with m^6A nucleotide solution and purified with an Oligo Clean & Concentrator kit (Zymo).

2.14. Sucrose gradient centrifugation and polysome fractionation

Sucrose gradient centrifugation and polysome fractionation were performed as previously described [31]. Briefly, cells were lysed in

polysome cell extraction buffer (50 mM MOPS, 15 mM $MgCl_2$, 150 mM NaCl, 100 μg/ml cycloheximide, 0.5% Triton X-100, 1 mg/ml heparin, 200 U RNaseOUT, 2 mM PMSF, and 1 μM benzamine) on ice. Cellular debris was cleared by centrifugation at 13,000 ×*g* for 10 min at 4 °C. Extracts were loaded on a 10–50% sucrose gradient and centrifuged at 36,000 rpm for 2.5 h at 4 °C in an SW 41 Ti rotor (Beckman coulter). Then RNA in the polysome fraction was extracted for qRT-PCR.

2.15. Dual luciferase reporter assay

Cells were seeded into the individual wells of a 24-well plate and co-transfected with vectors according to the Lipofectamine®3000 reagent (Invitrogen) protocol. After 48 h, the firefly and Renilla luciferase activities were measured by a Dual Luciferase Reporter Assay System (Promega). The relative luciferase activities were assessed in a SYNERGY microplate reader (BioTek). Each group was analysed in triplicate.

2.16. RNA immunoprecipitation (RIP)

RIP assays were performed as according to the manufacturer's instructions with Magna RIP™ RNA-Binding Protein Immunoprecipitation Kit (Millipore, USA). Normal rabbit IgG was used as the negative control, and anti-SNRNP70 was used as the positive control. Finally, the isolated RNA was analysed by qRT-PCR, and the isolated protein was analysed by Western blotting.

2.17. siRNA transfection

The siRNA used in this paper was synthesized by Sangon Biotech (Shanghai), and the siRNA oligonucleotide sequences are shown in Table S3. The synthesized siRNA was added to RNase-free water to prepare a 10 μM solution. Target cells were transiently transfected with Lipofectamine® RNAiMAX transfection reagent (Invitrogen) according to the instructions.

2.18. Sphere formation assay

Single-cell suspensions of cancer cells were plated in 60 mm ultra-low attachment culture dishes (Corning) at 12000 cells per well in sphere formation medium (serum-free RPMI 1640 medium containing 1× B-27(Gibco), 40 ng/ml EGF (Pepro Tech), and 20 ng/ml bFGF (Pepro Tech). On the third day, the culture medium was completely aspirated into a centrifuge tube, and centrifuged at 1000 rpm for 3 min, and the supernatant was then discarded. The cells were resuspended by adding fresh sphere formation medium. Three-dimensional tumour spheres growing from non-adherent clones were observed on the 7th day of culture. Tumour spheres with a diameter of ≥50.0 μm were counted. The sphere formation efficiency (SFE) was calculated using the following equation: SFE (%) = (# of spheres per well)/(# of cells seeded per well) × 100%.

2.19. Nude mouse subcutaneous transplantation tumour model and in vivo cancer metastasis model

All animal experimental procedures were approved by the Institutional Ethics Committee for Clinical Research and Animal Trials of the First Affiliated Hospital of Sun Yat-sen University. For the subcutaneous implantation model, 1×10^7 cells were subcutaneously implanted into 5-week-old BALB/cJNju-Foxn1nu/Nju nude mice (Nanjing Biomedical Research Institute of Nanjing University). Mice were sacrificed 4 weeks after subcutaneous implantation. Tumour formation and growth were assessed weekly. Tumour volume was calculated as follows: tumour volume = $1/2 \times a \times b^2$, where a = length, and b = width. For the cancer metastasis model, 1×10^6 cells were introduced into 5-week-old nude mice of the same strain by tail vein injection. Six weeks after injection, lung metastases were observed.

2.20. Statistical analysis

Error bars denote standard deviations (SDs) or standard errors of the mean (SEMs). Two groups of independent samples were compared by Student's *t*-test. The results of the cell l proliferation and cell migration experiments were analysed using repeated measure ANOVA. Protein expression data for bladder cancer clinical tissue sections were analysed using the Chi-square test. Pearson correlation was used for correlation analysis. ITGA6-related survival rate data were compared using the log-rank test. For a test with a size of $\alpha = 0.05$, $p < .05$ was considered statistically significant ($^*p < .05$, $^{**}p < .01$, $^{***}p < .001$, $^{****}p < .001$).

3. Results

3.1. METTL3 or ALKBH5 affected cell adhesion by regulating ITGA6 expression in BC cells

The change in tumour cell adhesion is one of the critical factors during oncogenesis. To study the role of the m^6A pathway in BC development and progression, we first examined whether BC cell adhesion was affected by the m^6A writer METTL3 and eraser ALKBH5. Our results revealed that depletion of METTL3 or overexpression of ALKBH5 in T24 and UM-UC-3 bladder cancer cells resulted in decreased cell adhesion (Fig. 1a–d). However, forced expression of METTL3 in human uroepithelial SV-HUC-1 cells strongly increased cell adhesion compared with that of control cells (Fig. 1e). In addition, depletion of ALKBH5 promoted cell adhesion in SV-HUC-1 cells (Fig. 1f). These results indicated that m^6A modifying enzymes regulate cell adhesion, with the m^6A writer METTL3 promoting but ALKBH5 inhibiting cell adhesion. To identify the direct targets of METTL3 and ALKBH5 involved in cell adhesion, we examined the protein expression of a panel of adhesion molecules in METTL3- or ALKBH5-modified BC and uroepithelial SV-HUC-1 cells. We found that either forced expression of METTL3 or depletion of ALKBH5 resulted in increased ITGA6 protein levels in SV-HUC-1 cells as detected by Western blotting. However, the ITGA6 mRNA levels were not concomitantly increased (Fig. 1g, h, m). Conversely, depletion of METTL3 in T24 and UM-UC-3 cells significantly reduced the expression of the ITGA6 protein without affecting mRNA expression (Fig. 1i,j,m). We also measured the expression of the ITGA6 protein in various stable cell lines by flow cytometric analysis, and obtained results similar to those of Western blotting (Additional file 1: Fig. S1a–d), suggesting that ITGA6 is an important adhesion molecule regulated by METTL3 and ALKBH5. Furthermore, we rescued METTL3/ALKBH5 expression in the same cell types to validate the influence of these enzymes on cell adhesion and ITGA6 expression and found that rescue of METTL3/ALKBH5 expression regulated ITGA6 expression and cell adhesion (Additional file 1: Fig.S2a–c). Overall, our data indicated that METTL3 and ALKBH5 affected cell adhesion by regulating ITGA6 protein expression in BC cells.

3.2. ITGA6 was significantly upregulated in BC and correlated with the prognosis of BC patients

Previous studies showed that METTL3 expression is upregulated in multiple types of cancers [18,20,32]. Given that METTL3 acts as an m^6A writer and regulates ITGA6 expression, we measured METTL3 and ITGA6 expression in bladder cancer cell lines and tissue microarrays. The results showed that METTL3 and ITGA6 protein were expressed at a significantly higher level in bladder cancer cell lines (T24, UM-UC-3, 5637, and J82) than in human uroepithelial SV-HUC-1 cells (Fig. 2a,b, Additional file 1: Fig. S1e). However, the expression of ITGA6 mRNA did not significantly differ in the above cells (Fig. 2c), suggesting the post-transcriptional regulation of ITGA6 expression in BC

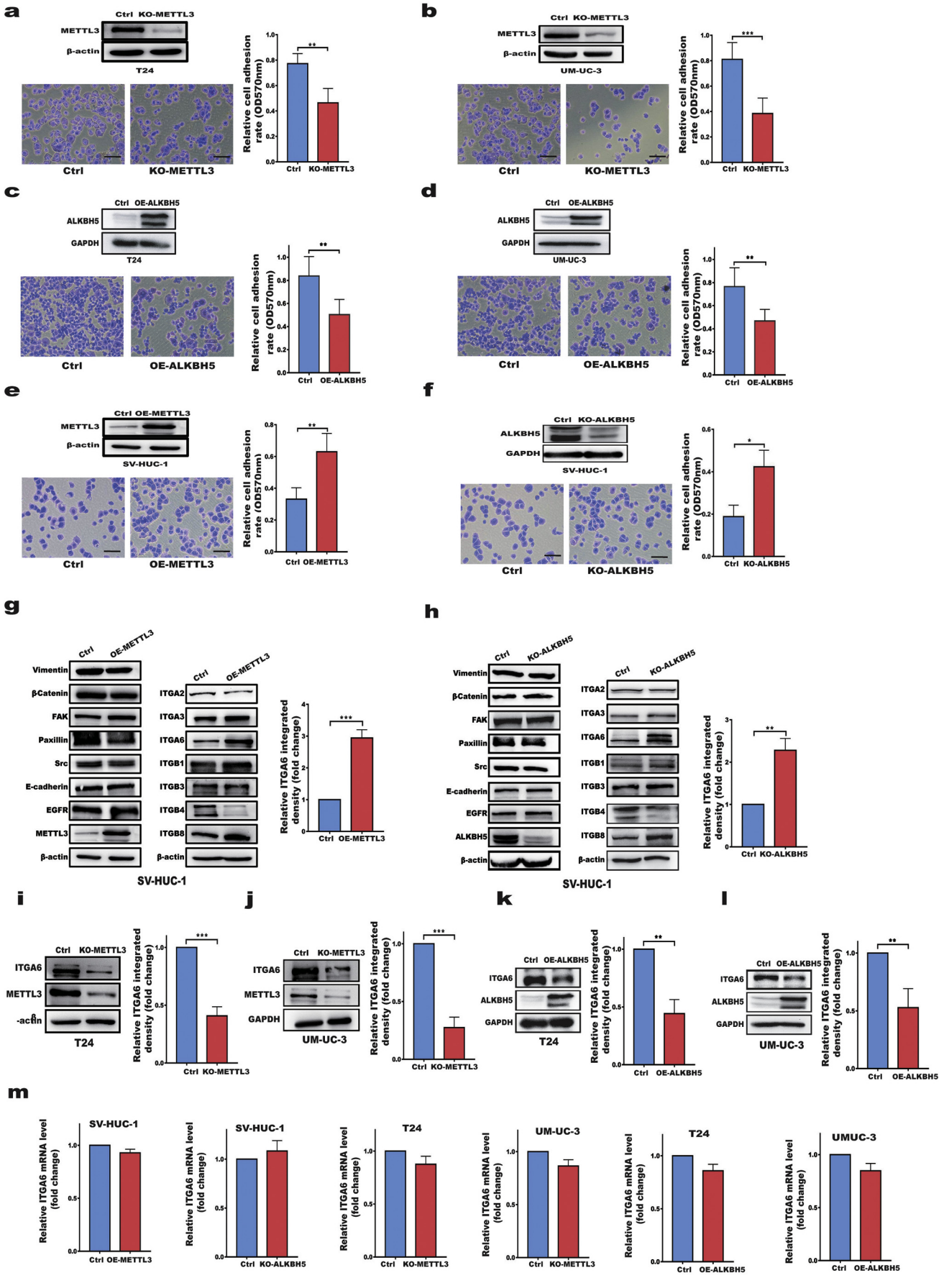
a
Ctrl KO-METTL3
METTL3
β-actin
T24
Ctrl
KO-METTL3
Relative cell adhesion rate (OD570nm)
Ctrl KO-METTL3
b
UM-UC-3
c
Ctrl OE-ALKBH5
ALKBH5
GAPDH
OE-ALKBH5
d
e
Ctrl OE-METTL3
SV-HUC-1
OE-METTL3
f
Ctrl KO-ALKBH5
KO-ALKBH5
g
Vimentin
βCatenin
FAK
Paxillin
Src
E-cadherin
EGFR
ITGA2
ITGA3
ITGA6
ITGB1
ITGB3
ITGB4
ITGB8
Relative ITGA6 integrated density (fold change)
h
i
ITGA6
-actin
j
k
l
m
Relative ITGA6 mRNA level (fold change)
SV-HUC-1
T24
UM-UC-3
UMUC-3

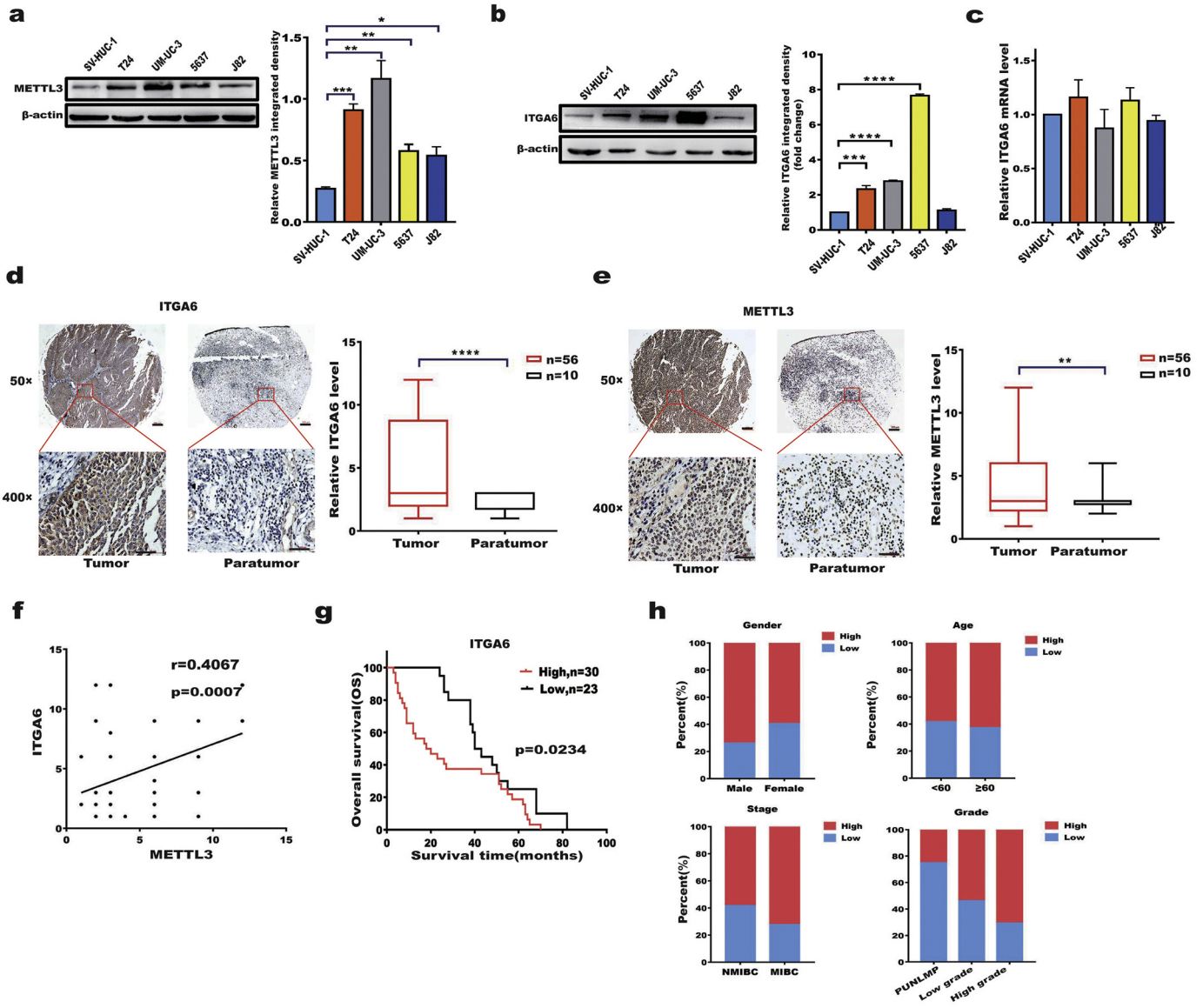

Fig. 2. ITGA6 was significantly upregulated in BC and correlated with the prognosis of BC patients. a, b Western blotting (left) of METTL3 (a) and ITGA6 (b) in bladder cancer cells. The chart (right) shows the relative ITGA6 integrated density in the Western blotting results. * $p < .05$, ** $p < .01$, *** $p < .001$, **** $p < .0001$. (one-way ANOVA, Dunnett 's test). c RT-qPCR analysis of ITGA6 mRNA expression in bladder cancer cells compared with that in SV-HUC-1 cells. d, e ITGA6 (d) and METTL3 (e) expression in bladder cancer patient tumour microarrays (TMAs). Representative images of IHC staining for ITGA6 and METTL3 in tumour and paratumour tissues of TMAs. Bar = 200 μm, 50×. Bar = 50 μm, 400×. The graph (right) shows that ITGA6 and METTL3 were significantly upregulated in bladder cancer TMAs. Tumour, $n = 56$. Paratumour, $n = 10$. ** $p < .01$, **** $p < .0001$. (Student's t-test). f Correlation analysis of ITGA6 and METTL3 expression in tissue microarrays; $r = 0.4067$, $p = .0007$. (Pearson's correlation analysis). g The Kaplan-Meier survival curve indicates that patients with high ITGA6 expression had low survival rates. h IHC staining of bladder cancer patient tumour samples revealed that the level of ITGA6 expression was positively correlated with histological grade and stage. The chart shows the statistical analysis of ITGA6 in bladder cancer clinical pathology sections. PUNLMP (papillary urothelial neoplasms of low malignant potential) = 4, Low-grade = 80, High-grade = 102. All bar plot data are the means ± SEMs of three independent experiments.

cells. Additionally, we used patient samples to evaluated the clinical relevance of ITGA6 expression in bladder cancer. Immunohistochemical (IHC) staining of BC tissue microarrays revealed that ITGA6 and METTL3 expression was moderate or high in most of the bladder cancer samples, but weak or not detectable in the majority of the paratumour controls (Fig. 2d, e). Moreover, analysis of the IHC staining showed that the expression of ITGA6 was highly correlated with that of METTL3 in human tissue microarrays (Fig. 2f) and that a higher expression level of ITGA6 in patients indicated a lower survival rate (Fig. 2g). Furthermore, we found that the level of ITGA6 expression was positively correlated with histological grade and stage in bladder cancer patient tumour samples ($p = .001$) (Fig. 2h, Table 1). From these collective results, we conclude that the expression of ITGA6 was upregulated and led to a worse prognosis in BC patients.

Fig. 1. METTL3 and ALKBH5 affected cell adhesion by regulating ITGA6 expression in BC cells. a, b Depletion of METTL3 (KO-METTL3) decreased the adhesion of T24 (a) or UM-UC-3 (b) cells. c Overexpression of METTL3 (OE-METTL3) enhanced the adhesion of SV-HUC-1 cells. d Depletion of ALKBH5 (KO-ALKBH5) enhanced the adhesion of SV-HUC-1 cells. e, f Overexpression of ALKBH5 (OE-ALKBH5) enhanced the adhesion of T24 (e) or UM-UC-3 (f) cells. g, h Western blotting of 14 cell adhesion molecules in OE-METTL3 (g) or KO-ALKBH5 (h) SV-HUC-1 cells. The chart (right) shows the relative ITGA6 integrated density in the Western blotting results. I, j Western blotting of ITGA6 in KO-METTL3 T24 (i) or KO-METTL3 UM-UC-3 (j) cells. The chart (right) shows the relative ITGA6 integrated density in the Western blotting results. K, l Western blotting of ITGA6 in OE-ALKBH5 T24 (k) or OE-ALKBH5 UM-UC-3 (l) cells. The chart (right) shows the relative ITGA6 integrated density in the Western blotting results. m RT-qPCR analysis of ITGA6 mRNA expression in stable cell lines. All bar plot data are the means ± SDs or means ± SEMs of three independent biological replicates. *$p < .05$, ** $p < .01$, *** $p < .001$, (Student's t-test).

Table 1
Correlation expression of ITGA6 and clinicopathological variables in186 cases of BC.

Cases	Feature	ITGA6		N	*p*-Value
		Low	High		
Gender	Male	39 (26.2%)	110 (73.8%)	149	>0.05 (0.0849)
	Female	15 (40.5%)	22 (59.5%)	37	
Age	<60	33 (41.8%)	46 (58.2%)	79	>0.05 (0.5446)
	≥60	40 (37.4%)	67 (62.6%)	107	
Stage	NMIBC (Ta/T1/Tis)	40 (41.7%)	56 (58.3%)	96	<0.05 (0.0471)
	MIBC (T2-T4)	25 (27.8%)	65 (72.2%)	90	
Grade	PUNLMP	3 (75.0%)	1 (25.0%)	4	<0.05 (0.0198)
	Low grade	37 (46.3%)	43 (53.7%)	80	
	High grade	30 (29.4%)	72 (70.6%)	102	

3.3. METTL3 and ALKBH5 reciprocally regulate ITGA6 mRNA m^{6}A modification and translation

To explore the molecular mechanisms underlying the METTL3- or ALKBH5-mediated regulation of ITGA6, we first determined whether m^{6}A modification exists in ITGA6 mRNA. By analysing our previous methylated RNA immunoprecipitation combined with RNA sequencing (MeRIP-seq) data from SV-HUC-1 cells, we identified the m^{6}A peak region located in the 3′UTR of ITGA6 (Fig. 3a). Moreover, Methyl Transcriptome DataBase (MeT-DB) [33] analysis of ITGA6 indicated that the m^{6}A methylation sites were mainly in the 3′UTR region of ITGA6 mRNA (Additional file 1: Fig. S3). To verify that m^{6}A-modified ITGA6 is regulated by METTL3 and ALKBH5, we performed MeRIP-qPCR experiments in METTL3-depleted T24 cells and in METTL3-overexpressing or ALKBH5-depleted SV-HUC-1 cells. The results showed that depletion of METTL3 significantly decreased the m^{6}A modification in the ITGA6 mRNA 3′UTR (Fig. 3b). Conversely, either METTL3 overexpression or ALKBH5 depletion significantly promoted m^{6}A modification in the ITGA6 mRNA 3′UTR (Fig. 3c). To determine whether the stability of ITGA6 mRNA is affected by m^{6}A, we conducted RNA stability assays and found that overexpression of METTL3 or depletion of ALKBH5 had little effect on the stability of ITGA6 mRNA (Fig. 3d, e). To assess the potential effects of METTL3 on ITGA6 protein stability, we treated cells with cycloheximide (CHX) to block translation and measured ITGA6 degradation. As shown in Fig. 3f and g, the degradation rates of the ITGA6 protein were clearly unchanged in either

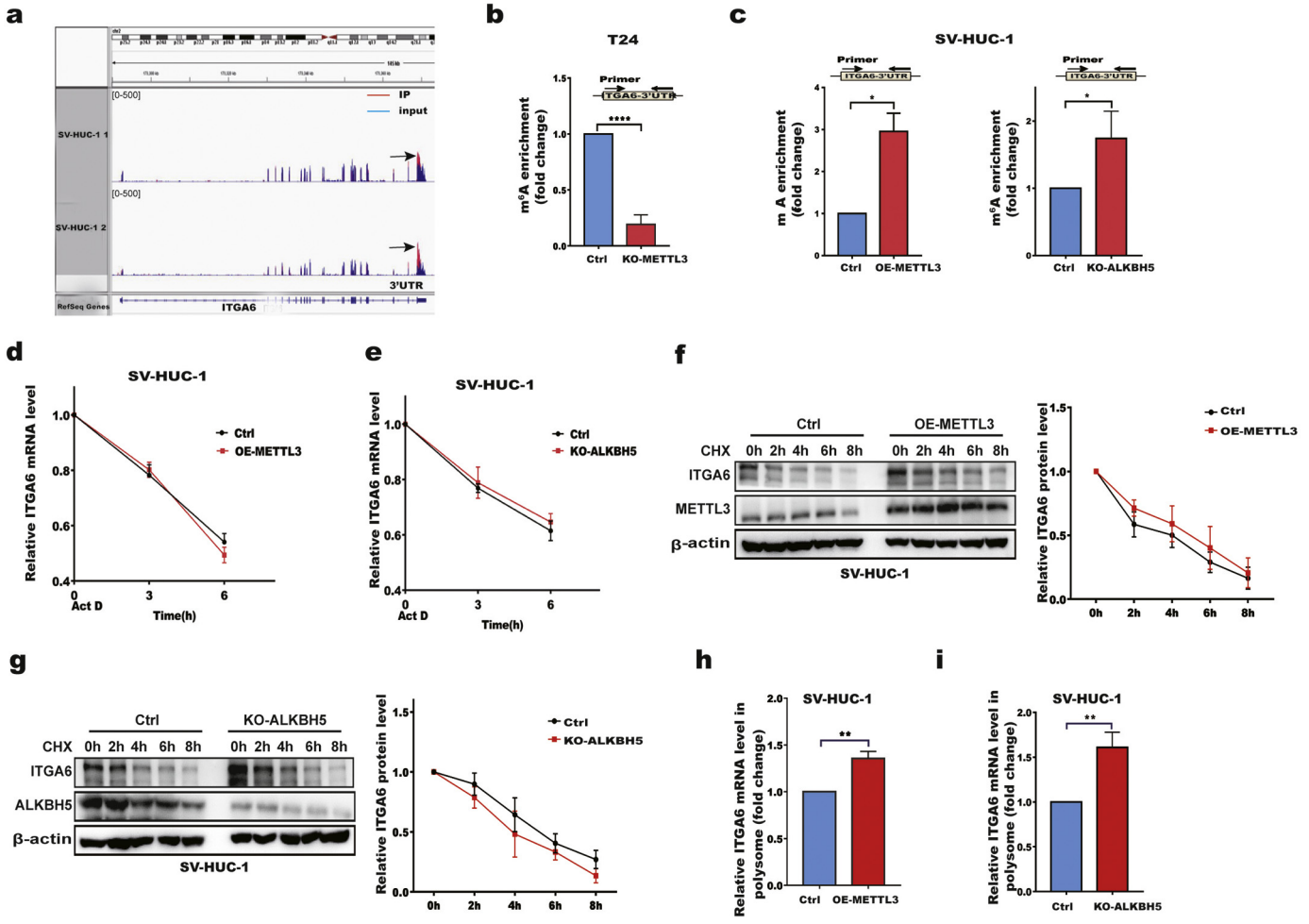

Fig. 3. METTL3 and ALKBH5 regulate ITGA6 mRNA m^{6}A modification and translation. a m^{6}A sites in the ITGA6 mRNA 3′UTR are shown from the of MeRIP-Seq data in SV-HUC-1 cells. b m^{6}A enrichment in the ITGA6 mRNA 3′UTR was validated by MeRIP-qPCR in control and KO-METTL3 T24 cells. c m^{6}A enrichment in the ITGA6 mRNA 3′UTR was validated by MeRIP-qPCR in control, OE-METTL3 and KO-ALKBH5 SV-HUC-1 cells. d, e ITGA6 mRNA stability in control, OE-METTL3 (d), and KO-ALKBH5 (e) SV-HUC-1 cells. RT-qPCR analysis of ITGA6 mRNA at the indicated time points after treatment with actinomycin D (Act D). f, g ITGA6 protein stability in control, OE-METTL3 (f), and KO-ALKBH5 (g) SV-HUC-1 cells. Western blotting of ITGA6 at the indicated time points after treatment with cycloheximide (CHX). h, i RT-qPCR analysis of the ITGA6 mRNA abundance in polysome fractions collected by sucrose gradient centrifugation in control, OE-METTL3 (h), and KO-ALKBH5 (i) SV-HUC-1 cells. All bar plot data are the means ± SEMs of three independent experiments except in (b, c), where the error bars denote the SDs of technical triplicates. $^*p < .05$, $^{**}p < .01$, $^{****}p < .0001$. (Student's *t*-test).

METTL3-overexpressing or ALKBH5-depleted SV-HUC-1 cells compared with those in control cells. We then compared the polysome-bound (translationally active) ITGA6 mRNA levels in METTL3-overexpressing or ALKBH5-depleted cells with those in control cells. The results showed that the polysome-bound ITGA6 mRNA levels were significantly increased in METTL3-overexpressing or ALKBH5-depleted SV-HUC-1 cells compared with those in control cells (Fig. 3h, i). In contrast, depletion of METTL3 in T24 cells significantly reduced the proportion of ITGA6 transcripts in the polysome fractions, suggesting that METTL3 enhances the proportion of ITGA6 mRNAs undergoing active translation (Additional file 1: Fig. S4a). Overall, our data indicated that METTL3 and ALKBH5 reciprocally act on the 3′UTR of ITGA6 mRNA for m^{6}A modification and translation.

3.4. m^{6}A motifs within the 3′ UTR of ITGA6 promote ITGA6 mRNA translation

To elucidate the molecular mechanisms underlying the m^{6}A-mediated translation of ITGA6 mRNA, we first extracted m^{6}A modifications from GEO datasets and found the 4 m^{6}A motifs within the 3′UTR of ITGA6 at a single-nucleotide resolution by retrieving data from m^{6}A iCLIP (miCLIP)-Seq in CD8 T cells and A549 cells (Additional file 1: Fig. S5a) [34]. We then cloned the ITGA6 3′UTR region, including fragments with the 4 wild-type m^{6}A motifs (WT) or mutant (A-to-T mutation) m^{6}A sites into a luciferase reporter vector to determine the function of these m^{6}A motifs in the regulation of ITGA6 translation (Fig. 4a). As shown in Fig. 4b and4c, ectopically expressed METTL3

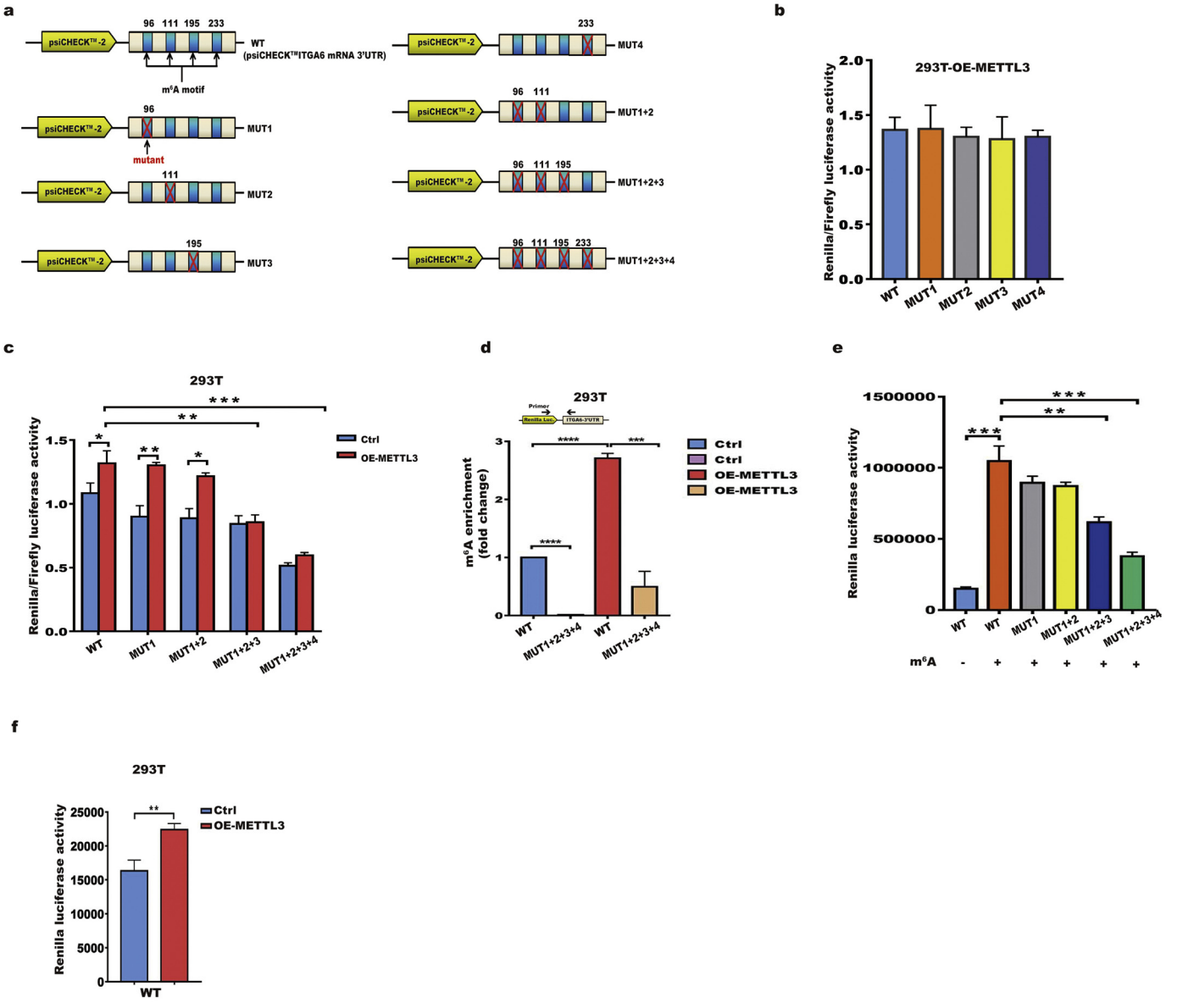

Fig. 4. m^{6}A motifs within the 3′UTR of ITGA6 promote the translation of ITGA6 mRNA. a psiCHECK™-2 luciferase reporter constructs containing fragments of the human ITGA6 3′UTR with 4 putative wild-type m^{6}A motifs (WT) or mutant (A-to-T mutation) m^{6}A sites (MUT1, MUT2, MUT3, MUT4, MUT1 + 2, MUT1 + 2 + 3, or MUT1 + 2 + 3 + 4) are shown. The position of the m^{6}A sites (96, 111, 195, and 233) is numbered relative to the first nucleotide of the 3′UTR. b Relative luciferase activity of the psiCHECK™-2-ITGA6 3′UTR with either wild-type (WT) or single mutation of m^{6}A sites 1, 2, 3, or 4 (MUT1, MUT2, MUT3, or MUT4) in METTL3-overexpressing 293 T cells. Renilla luciferase activity was measured and normalized to firefly luciferase activity. c Relative luciferase activity of psiCHECK™-2-ITGA6 3′UTR with either wild-type (WT) or mutant m^{6}A sites (MUT1, MUT1 + 2, MUT1 + 2 + 3, or MUT1 + 2 + 3 + 4) in control and METTL3-overexpressing 293 T cells. Renilla luciferase activity was measured and normalized to firefly luciferase activity. d m^{6}A enrichment in the psiCHECK™-2-ITGA6 mRNA 3′UTR was validated by MeRIP-qPCR in control and OE-METTL3 293T cells after transfection of the WT and MUT1 + 2 + 3 + 4 plasmids. The primer covers the junction between Renilla Luc and the ITGA6 3′UTR. e Renilla luciferase activity was detected *in vitro* using the Flexi Rabbit Reticulocyte Lysate System. Renilla luciferase reporter mRNAs with the ITGA6 3′UTR (WT, MUT1, MUT1 + 2, MUT1 + 2 + 3, or MUT1 + 2 + 3 + 4) were transcribed *in vitro* in the absence or presence of m^{6}A. All bar plot data are the means ± SEMs of three independent experiments except in (c), where the error bars denote the SDs of technical triplicates. *$p < .05$, **$p < .01$, ***$p < .001$, ****$p < .0001$. (Student's *t*-test, one-way ANOVA, Dunnett 's test).

promoted the activity of the luciferase construct containing the ITGA6 3′ UTR. However, mutation of any of the four sites (MUT1, MUT2, MUT3, or MUT4) did not significantly change METTL3-augmented translation of the luciferase reporter. Furthermore, mutation of the first or first two m6A motifs (MUT1 or MUT1 + 2, respectively) slightly decreased METTL3's effects on translation, while mutations of the first three or all four motifs (MUT1 + 2 + 3 or MUT1 + 2 + 3 + 4, respectively) completely abolished METTL3-augmented translation of the luciferase reporter (Fig. 4c, Additional file 1: Fig. S5b), suggesting that the m^{6}A motifs 1–3 together are essential for METTL3-augmented ITGA6 expression. To further validate whether the above effects are related to m^{6}A modifications, we conducted gene-specific m^{6}A qPCR on the cloned wild-type and mutant 3′UTR fragments of the ITGA6 gene (WT and MUT1 + 2 + 3 + 4, respectively) in the 293T cells that were used for the luciferase reporter assays. As expected, the WT fragment had a high abundance of m^{6}A, whereas the MUT1 + 2 + 3 + 4 fragment contained no or minimal levels of m^{6}A. Forced expression of METTL3 significantly increased the m^{6}A abundance in the WT 3′UTR fragment of ITGA6 (Fig. 4d). Moreover, *in vitro* translation using the control and m^{6}A modified reporter mRNAs further confirmed the role of m^{6}A modification in promoting ITGA6 translation (Fig. 4e,f). Overall, the above results further demonstrated that the m^{6}A modifications in the ITGA6 3′UTR promote the translation of ITGA6 mRNA.

3.5. YTHDF1/YTHDF3 preferentially recognizes m^{6}A residues in the ITGA6 3′ UTR and promotes ITGA6 translation

A group of YT521-B homology (YTH) domain-containing proteins (YTHDFs) are well established m^{6}A readers, each of which recognizes a few thousands of methylated transcripts in mammalian cells. To determine which m^{6}A reader is involved in promoting ITGA6 translation, we investigated the effect of YTHDF1-YTHDF3 silencing by RNAi on ITGA6 expression. The results showed that silencing YTHDF1 or YTHDF3 but not YTHDF2 significantly decreased ITGA6 expression (Fig. 5a). Moreover, forced expression of YTHDF1/YTHDF3 significantly promoted ITGA6 expression (Fig. 5b,c). Next, we investigated whether

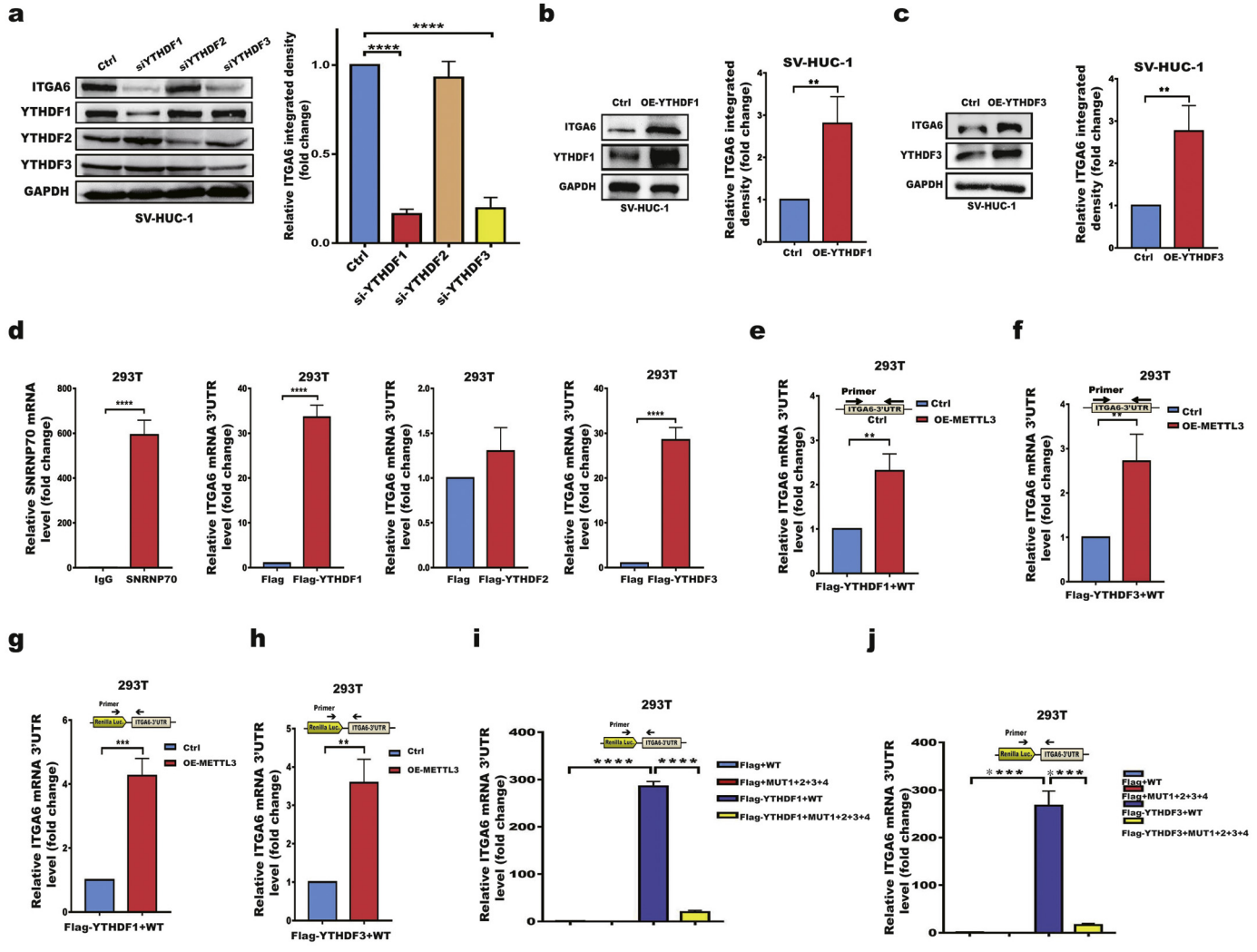

Fig. 5. YTHDF1/YTHDF3 preferentially recognize m^{6}A residues in the ITGA6 3′UTR and promote ITGA6 translation. a Western blotting of ITGA6 expression in SV-HUC-1 cells treated with control or YTHDF1, YTHDF2, or YTHDF3 siRNAs. b, c Western blotting of ITGA6 in OE-YTHDF1 (b) or OE-YTHDF3 (c) SV-HUC-1 cells. d RIP analysis of the binding of the YTHDF1, YTHDF2, or YTHDF3 proteins to ITGA6 mRNA in 293T cells. FLAG-tagged YTHDF1, YTHDF2, YTHDF3 or control 2AB vectors were transfected into 293T cells. Lysates were immunoprecipitated with an anti-FLAG antibody. Enrichment of the ITGA6 mRNA 3′UTR with FLAG was measured by RT-qPCR and normalized to input. IgG, negative control, SNRNP70, positive control. e, f RIP analysis of the binding of the YTHDF1 (e) and YTHDF3 (f) proteins to ITGA6 mRNA in METTL3-overexpressing and control 293T cells g, h RIP analysis of the binding of the YTHDF1 (g) and YTHDF3 (h) proteins to exogenous ITGA6 mRNA 3′UTR. Both stable METTL3-overexpressing and control 293T cells were transfected with psiCHECK™-2-ITGA6 mRNA 3′UTR (WT) and FLAG-tagged YTHDF1, YTHDF3 or control 2AB vectors. Enrichment of the psiCHECK™-2-ITGA6 mRNA 3′UTR with FLAG was measured by RT-qPCR and normalized to input. The primer covers the junction between Renilla Luc and the ITGA6 3′UTR. i, j RIP analysis of the binding of the YTHDF1 (i) and YTHDF3 (j) proteins to exogenous ITGA6 mRNA 3′UTR containing wild-type m6A sites (WT) and 4 mutated m6A sites (MUT1 + 2 + 3 + 4). All bar plot data are the means ± SEMs of three independent experiments. $^{**}p < .01$, $^{***}p < .001$, $^{****}p < .0001$. (Student's *t*-test, one-way ANOVA, Dunnett's test).

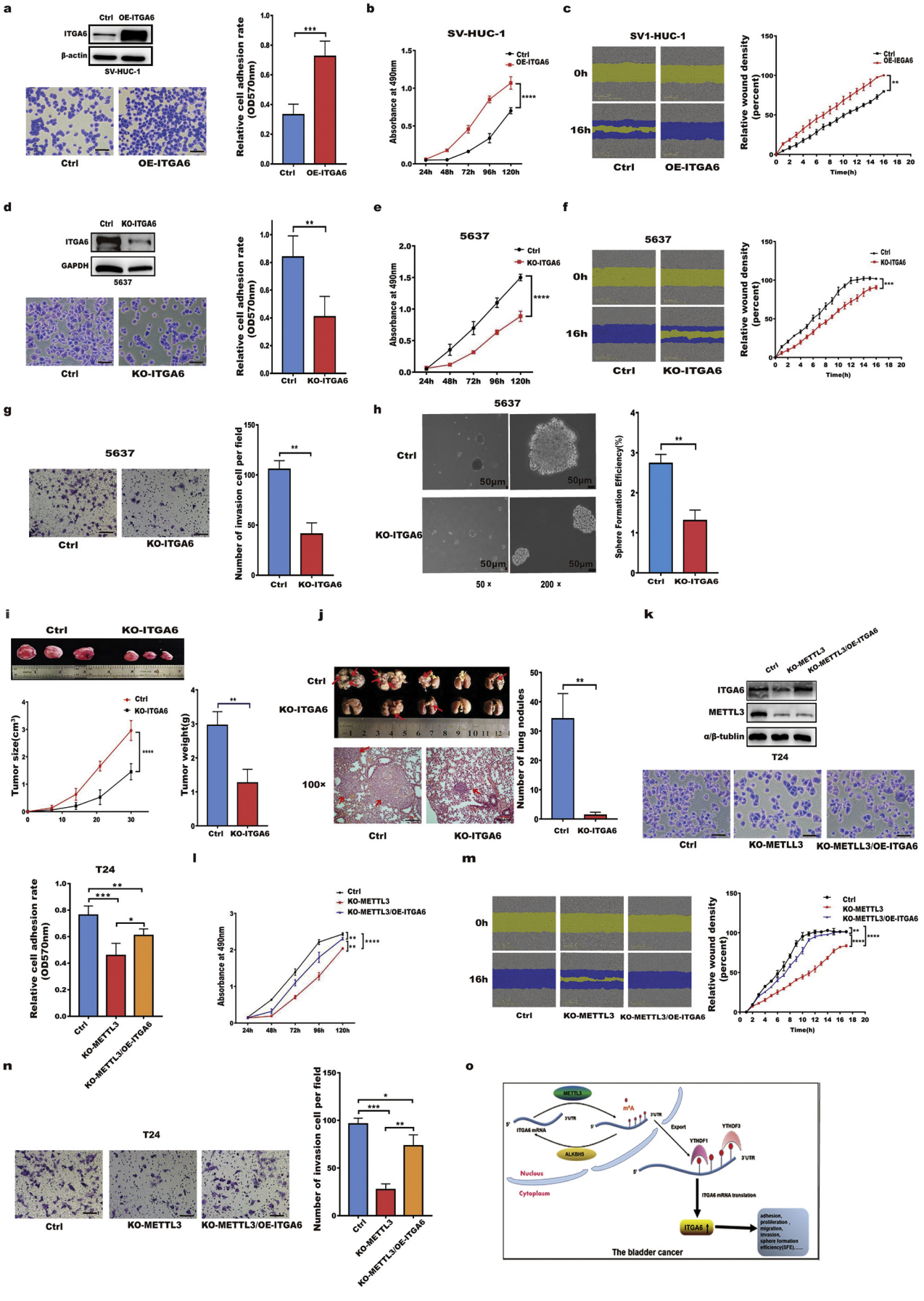
a
Ctrl OE-ITGA6
ITGA6
β-actin
SV-HUC-1
Ctrl
OE-ITGA6
Relative cell adhesion rate (OD570nm)
***
b
SV-HUC-1
Absorbance at 490nm
Ctrl
OE-ITGA6
****
24h 48h 72h 96h 120h
c
SV1-HUC-1
0h
16h
Ctrl
OE-ITGA6
Relative wound density (percent)
Time(h)
d
Ctrl KO-ITGA6
ITGA6
GAPDH
5637
Ctrl
KO-ITGA6
Relative cell adhesion rate (OD570nm)
**
e
5637
Absorbance at 490nm
Ctrl
KO-ITGA6
****
24h 48h 72h 96h 120h
f
5637
0h
16h
Ctrl
KO-ITGA6
Relative wound density (percent)
Time(h)
g
5637
Ctrl
KO-ITGA6
Number of invasion cell per field
h
5637
Ctrl
KO-ITGA6
50μm
50 ×
200 ×
Sphere Formation Efficiency(%)
i
Ctrl
KO-ITGA6
Tumor size(cm³)
Tumor weight(g)
j
Ctrl
KO-ITGA6
100×
Number of lung nodules
k
Ctrl
KO-METTL3
KO-METTL3/OE-ITGA6
ITGA6
METTL3
α/β-tublin
T24
KO-METLL3
KO-METLL3/OE-ITGA6
l
T24
Relative cell adhesion rate (OD570nm)
KO-METTL3
KO-METTL3/OE-ITGA6
Absorbance at 490nm
m
0h
16h
Relative wound density (percent)
Time(h)
n
T24
Number of invasion cell per field
o
METTL3
m⁶A
ITGA6 mRNA
5'UTR
3'UTR
Export
YTHDF3
YTHDF1
ALKBH5
Nucleus
Cytoplasm
ITGA6 mRNA translation
ITGA6
adhesion, proliferation, migration, invasion, sphere formation efficiency(SFE).....
The bladder cancer

the YTHDF1 and YTHDF3 proteins can bind to the ITGA6 3′UTR. As shown in Fig. 5d, Flag-tagged YTHDF1/YTHDF3 but not YTHDF2 selectively bound to ITGA6 mRNA. Moreover, overexpression of METTL3 significantly enhanced the interaction between YTHDF1/YTHDF3 and ITGA6 mRNA (Fig. 5e, f), suggesting that METTL3 facilitates the binding of YTHDF1/YTHDF3 to ITGA6 mRNA by mediating m^{6}A modification. Consistent with the findings for endogenous ITGA6 mRNA, the YTHDF1/YTHDF3 proteins interacted with ITGA6 reporter mRNA, and forced expression of METTL3 promoted the binding of YTHDF1/YTHDF3 to ITGA6 reporter mRNA (Fig. 5g, h). Moreover, YTHDF1/YTHDF3 interacts only with the WT ITGA6 reporter mRNA, not the m^{6}A motif-mutated mRNA (Fig. 5i, j; Additional file 1: Fig. S6). Collectively, our data revealed that the binding of YTHDF1/YTHDF3 to the m^{6}A motifs in the ITGA6 3′UTR promotes ITGA6 translation.

3.6. ITGA6 promoted the growth and progression of bladder cancer cells in vitro and in vivo

We further investigated the role of ITGA6 in BC growth and metastasis by establishing cell lines with stable ITGA6expression or depletion. As shown in Fig. 6a–c, ITGA6 overexpression significantly increased the adhesion, proliferation and migration of SV-HUC-1 uroepithelial cells. Conversely, depletion of ITGA6 in T24 and 5637 cells significantly suppressed the adhesion, proliferation, migration, invasion and sphere formation efficiency (SFE) (Fig. 6d–h; Additional file 1: Fig. S7). To verify the function of ITGA6 *in vivo*, we subcutaneously injected nude mice with ITGA6-depleted T24 cells and found that depletion of ITGA6 significantly slowed tumour growth (Fig. 6i). Moreover, we established a lung metastasis model by injecting tumour cells into the tail vein of nude mice to assess the role of ITGA6 in tumour metastasis. Many fewer micrometastases were found in the lungs of mice in the ITGA6-depleted group (Fig. 6j), implying that depletion of ITGA6 could inhibit tumour lung metastasis *in vivo*. Collectively, our data revealed that ITGA6 enhances the growth and metastatic capacity of BC cells.

3.7. Overexpression of ITGA6 in METTL3-deleted cells partially restored cell phenotypes

To further define whether ITGA6 is a direct effector of METTL3 in BC development, we performed a rescue experiment by overexpressing ITGA6 in METTL3-depleted cells in which ITGA6 was downregulated. As shown in Fig. 6k–n, forced expression of ITGA6 partially reversed the effects of METTL3-depletion on adhesion, proliferation, migration and invasion in T24 cells. Consistent with these findings, ITGA6 overexpression also reversed the phenotype caused by METTL3 deficiency in UM-UC-3 cells (Additional file 1: Fig. S8). Taken together, these data indicated that ITGA6 as an oncogenic factor is a functionally critical target of METTL3 in BC.

4. Discussion

An increasing number of studies have shown that aberrant m^{6}A modification is closely related to the occurrence and development of various types of cancers [19,23,32,35,36]. Elucidation of the biological relevance of m^{6}A alterations in tumorigenesis is contingent on the identification of specific target loci and the delineation of the mechanisms regulating m^{6}A on specific genes. However, research on the role and mechanism of m^{6}A modifications in bladder cancer is still in its infancy. In the present study, we provide evidence that the m^{6}A writer METTL3 and eraser ALKBH5 modulate ITGA6 expression through m^{6}A-based post-transcriptional regulation; the m^{6}A readers YTHDF1/YTHDF3 preferentially recognize m^{6}A residues in the ITGA6 3′UTR and promote ITGA6 translation, revealing a novel regulatory pathway of m^{6}A-modified ITGA6 in BC. Importantly, we demonstrate ITGA6 as a critical downstream target of METTL3 in promoting the growth and progression of bladder cancer cells *in vitro* and *in vivo*. To f our knowledge, our study is the first to uncover the oncogenic function of m^{6}A-modified ITGA6 in the pathogenesis of human bladder cancer (Fig. 6o).

ITGA6 as a member of the Integrin family is a subunit of Integrin alpha 6, also known as CD49f, vla-6, or ITGA6B. Integrins not only mediate interactions with the ECM, but also drive intracellular signals that communicate from the tumour microenvironment to the tumour cell, leading to cell migration and invasion [37]. ITGA6 forms heterodimers with either ITGB4 (CD104) or ITGB1 (CD29) to generate α6β4 integrin or α6β1 integrin, respectively. Both of these integrins are cell adhesion molecules that are vital to signalling pathways that regulate tumour development, metastasis, and angiogenesis [38,39]. Several lines of evidence demonstrate that ITGA6 is a putative stemness marker [40–43], and aberrant expression of ITGA6 has been shown to play an important role in the development and progression of various types of cancers [29,44–46]. Notably, the expression of ITGA6 is significantly associated with the incidence of intravesical recurrence [47]. Moreover, ITGA6 has not only been identified in BC cell-derived extracellular vesicles (EVs) [48,49], but has also been identified as one of 18 genes that defined the "tumour differentiation signature" applied for BC stratification [50]. However, how ITGA6 is regulated in cancers has not been fully investigated, and its role in bladder cancer is largely unknown. In the present study, our data revealed that ITGA6 expression was moderate or high in most of the bladder cancer samples and that a higher expression level of ITGA6 in patients indicated a lower survival rate. Importantly, our study revealed that inhibition of ITGA6 resulted in decreased proliferation, migration and invasion of bladder cancer cells *in vitro* and *in vivo*, indicating that ITGA6 is essential for the growth and metastasis of bladder cancer cells.

ITGA6 has been shown to be regulated at multiple layers. Many transcription factors, including RUNX1, HIFs and FOSL1, bind to the ITGA6 promoter and enhance its transcription [27,51,52], while KLF9 represses the transcription of ITGA6 by binding its promoter region [53]. More recently, a study showed that MYC can directly control ITGA6 promoter activity in CRC cells, leading to overexpression of the pro-proliferative ITGA6A splice variant [54]. Additionally, several miRNAs have been identified to inhibit ITGA6 expression post-transcriptionally [44,55–57]. At the post-translational level, chronic hypoxia increases the cell surface localization of ITGA6 in a Rab11-dependent manner, and promotes invasion in MDA-MB-231 cells [58]. Here, we found that highly enriched m^{6}A in the ITGA6 mRNA 3′UTR promotes the translation of ITGA6 mRNA *via* binding of the m^{6}A readers YTHDF1 and YTHDF3 in BC, revealing a novel post-transcriptional, m^{6}A-dependent mechanism of ITGA6 expression.

Recently, a study showed that METTL3 promotes bladder cancer progression *via* the AFF4/NF-κB/MYC signalling network [59]. In addition, our m^{6}A MeRIP-seq screening and functional study identified the role of the METTL3/m^{6}A/CDCP1 axis in chemical-induced bladder cancer carcinogenesis and metastasis [26]. Indeed, thousands of genes

Fig. 6. ITGA6 promoted the growth and progression of bladder cancer cells *in vitro* and *in vivo*. a–c Effects of forced expression of ITGA6 on the adhesion (a), proliferation (b), and migration (c) of SV-HUC-1 cells. Bar = 100 μm, 200×. d–g Effects of ITGA6 knockout on the adhesion (d), proliferation (e), migration (f), and invasion (g) of 5637 cells. Bar = 100 μm, 200×. h Sphere formation assay to determine the SFE in control and ITGA6-depleted (KO-ITGA6) 5637 cells. Bar = 50 μm, 50× and 200×. i Subcutaneous tumour model of KO-ITGA6 T24 cells. Tumour images, growth curves, and weights at the endpoint are shown. j *In vivo* tumour metastasis model of KO-ITGA6 T24 cells. The graph represents the number of lung nodules. Formation of T24 cell metastatic foci in the lung was confirmed by H&E staining. Bar = 200 μm, 100×. k–n Effects of forced expression of ITGA6 in KO-METTL3 T24 cells. ITGA6 partially restored the cell adhesion (k), proliferation (l), migration (m), and invasion (n) capacities in T24 cells, which were reduced by METTL3 knockout. o The schematic model of the role and underlying mechanism of m^{6}A-mediated ITGA6 in bladder cancer development. All bar plot data are the means ± SDs or means ± SEMs of three independent biological replicates. $^*p < .05$, $^{**}p < .01$, $^{***}p < .001$, $^{****}p < .0001$. (Student's *t*-test, one-way ANOVA, Tukey's multiple comparisons test).

modified by m^{6}A have been identified; among these genes, numerous genes modified by m^{6}A, such as EGFR, BCL2, ASB2, SOCS2, FOXM1, Myc and PTEN, have been revealed to play regulatory roles in tumour formation and progression [17,20,23,35]. In the present study, we found that the adhesion molecule ITGA6 is another critical downstream molecule regulated by METTL3 or ALKBH5 through m^{6}A modification, implying that the m^{6}A modification pathway contributes to BC occurrence and progression probably through the regulation of distinct sets of target genes. Since the fates of m^{6}A-modified RNA transcripts are dependent on the types of m^{6}A readers that recognize the m^{6}A modification on the target gene, distinct m^{6}A modifications on target loci display different biological functions. Several studies have demonstrated that YTHDF2 accelerates the degradation of m^{6}A-modified transcripts [13], while YTHDF1 and YTHDF3 enhance the translation efficiency of m^{6}A-modified target RNAs [12,14,60]. Consistent with these results, our study revealed that YTHDF1 and YTHDF3 but not YTHDF2 preferentially recognize m^{6}A residues in the ITGA6 3′UTR and promote ITGA6 translation.

Overall, our study uncovers an oncogenic role of m^{6}A-modified ITGA6 and its regulatory mechanisms in BC development and progression, suggesting that m^{6}A-modified ITGA6 is a promising therapeutic target for the treatment of BC.

Funding sources

This work was supported by grants from the National Natural Science Foundation of China (No. 81772699, No. 81472999, No. 81272350), Key Natural Science Foundation of Guangdong (No.2015A030311038), Guangzhou People's Livelihood Science and Technology Project (201803010052), and National Key Research and Development Program of China (2016YFC1300600).

Declaration of Competing Interests

The authors declare no conflicts of interest.

Author contributions

HJ, XY, and BQ conceived and performed the experiments, analysed the data. HZ, ZY, YC, and DQ performed the experiments. XW, MY performed the bioinformatics analysis. WM, SL, and MY edited the manuscript. WJ conceived of the project, analysed data, wrote the manuscript, and provided supervision. WM provided critical reagents. All authors revised and edited the manuscript.

Acknowledgements

We thank the National Natural Science Foundation of China, Natural Science Foundation of Guangdong Province and Guangzhou Municipal Science and Technology Bureau for their financial support. The funders had no role in study design, data collection, data analysis, interpretation or writing of the report. We thank all members of the Wang labs for useful discussions.

Appendix A. Supplementary data

Supplementary data to this article can be found online at https://doi.org/10.1016/j.ebiom.2019.07.068.

References

[1] Bray F, Ferlay J, Soerjomataram I, Siegel RL, Torre LA, Jemal A. Global cancer statistics 2018: GLOBOCAN estimates of incidence and mortality worldwide for 36 cancers in 185 countries. CA Cancer J Clin 2018;68(6):394–424.
[2] Sylvester RJ, van der Meijden AP, Oosterlinck W, Witjes JA, Bouffioux C, Denis L, et al. Predicting recurrence and progression in individual patients with stage Ta T1 bladder cancer using EORTC risk tables: a combined analysis of 2596 patients from seven EORTC trials. Eur Urol 2006;49(3) [466–5; discussion 75-7].
[3] Antoni S, Ferlay J, Soerjomataram I, Znaor A, Jemal A, Bray F. Bladder cancer incidence and mortality: a global overview and recent trends. Eur Urol 2017;71(1):96–108.
[4] Katsila T, Liontos M, Patrinos GP, Bamias A, Kardamakis D. The new age of -omics in urothelial cancer - re-wording its diagnosis and treatment. EBioMedicine 2018;28:43–50.
[5] Peer E, Rechavi G, Dominissini D. Epitranscriptomics: regulation of mRNA metabolism through modifications. Curr Opin Chem Biol 2017;41:93–8.
[6] Bokar JA, Shambaugh ME, Polayes D, Matera AG, Rottman FM. Purification and cDNA cloning of the AdoMet-binding subunit of the human mRNA (N6-adenosine)-methyltransferase. Rna 1997;3(11):1233–47.
[7] Liu J, Yue Y, Han D, Wang X, Fu Y, Zhang L, et al. A METTL3-METTL14 complex mediates mammalian nuclear RNA N6-adenosine methylation. Nat Chem Biol 2014;10(2):93–5.
[8] Patil DP, Chen CK, Pickering BF, Chow A, Jackson C, Guttman M, et al. m(6)A RNA methylation promotes XIST-mediated transcriptional repression. Nature 2016;537(7620):369–73.
[9] Ping XL, Sun BF, Wang L, Xiao W, Yang X, Wang WJ, et al. Mammalian WTAP is a regulatory subunit of the RNA N6-methyladenosine methyltransferase. Cell Res 2014;24(2):177–89.
[10] Jia G, Fu Y, Zhao X, Dai Q, Zheng G, Yang Y, et al. N6-methyladenosine in nuclear RNA is a major substrate of the obesity-associated FTO. Nat Chem Biol 2011;7(12):885–7.
[11] Zheng G, Dahl JA, Niu Y, Fedorcsak P, Huang CM, Li CJ, et al. ALKBH5 is a mammalian RNA demethylase that impacts RNA metabolism and mouse fertility. Mol Cell 2013;49(1):18–29.
[12] Li A, Chen YS, Ping XL, Yang X, Xiao W, Yang Y, et al. Cytoplasmic m(6)A reader YTHDF3 promotes mRNA translation. Cell Res 2017;27(3):444–7.
[13] Wang X, Lu Z, Gomez A, Hon GC, Yue Y, Han D, et al. N6-methyladenosine-dependent regulation of messenger RNA stability. Nature 2014;505(7481):117–20.
[14] Wang X, Zhao BS, Roundtree IA, Lu Z, Han D, Ma H, et al. N(6)-methyladenosine modulates messenger RNA translation efficiency. Cell 2015;161(6):1388–99.
[15] Haussmann IU, Bodi Z, Sanchez-Moran E, Mongan NP, Archer N, Fray RG, et al. m(6)A potentiates Sxl alternative pre-mRNA splicing for robust Drosophila sex determination. Nature 2016;540(7632):301–4.
[16] Xiao W, Adhikari S, Dahal U, Chen YS, Hao YJ, Sun BF, et al. Nuclear m(6)A reader YTHDC1 regulates mRNA splicing. Mol Cell 2016;61(4):507–19.
[17] Chen M, Wei L, Law CT, Tsang FH, Shen J, Cheng CL, et al. RNA N6-methyladenosine methyltransferase-like 3 promotes liver cancer progression through YTHDF2-dependent posttranscriptional silencing of SOCS2. Hepatology 2018;67(6):2254–70.
[18] Choe J, Lin S, Zhang W, Liu Q, Wang L, Ramirez-Moya J, et al. mRNA circularization by METTL3-eIF3h enhances translation and promotes oncogenesis. Nature 2018;561(7724):556–60.
[19] Liu J, Eckert MA, Harada BT, Liu SM, Lu Z, Yu K, et al. m(6)A mRNA methylation regulates AKT activity to promote the proliferation and tumorigenicity of endometrial cancer. Nat Cell Biol 2018;20(9):1074–83.
[20] Vu LP, Pickering BF, Cheng Y, Zaccara S, Nguyen D, Minuesa G, et al. The N(6)-methyladenosine (m(6)A)-forming enzyme METTL3 controls myeloid differentiation of normal hematopoietic and leukemia cells. Nat Med 2017;23(11):1369–76.
[21] Weng H, Huang H, Wu H, Qin X, Zhao BS, Dong L, et al. METTL14 Inhibits Hematopoietic Stem/Progenitor Differentiation and Promotes Leukemogenesis via mRNA m(6)A Modification. Cell Stem Cell 2018;22(2):191–205 [e199].
[22] Zhang C, Samanta D, Lu H, Bullen JW, Zhang H, Chen I, et al. Hypoxia induces the breast cancer stem cell phenotype by HIF-dependent and ALKBH5-mediated m(6)A-demethylation of NANOG mRNA. Proc Natl Acad Sci U S A 2016;113(14):E2047–56.
[23] Zhang S, Zhao BS, Zhou A, Lin K, Zheng S, Lu Z, et al. m(6)A Demethylase ALKBH5 maintains tumorigenicity of glioblastoma stem-like Cells by Sustaining FOXM1 expression and cell proliferation program. Cancer Cell 2017;31(4):591–606 [e596].
[24] Deng X, Su R, Weng H, Huang H, Li Z, Chen J. RNA N(6)-methyladenosine modification in cancers: current status and perspectives. Cell Res 2018;28(5):507–17.
[25] Wang S, Chai P, Jia R, Jia R. Novel insights on m(6)A RNA methylation in tumorigenesis: a double-edged sword. Mol Cancer 2018;17(1):101.
[26] Yang F, Jin H, Que B, Chao Y, Zhang H, Ying X, et al. Dynamic m(6)A mRNA methylation reveals the role of METTL3-m(6)A-CDCP1 signaling axis in chemical carcinogenesis. Oncogene 2019;38(24):4755–72.
[27] Brooks DL, Schwab LP, Krutilina R, Parke DN, Sethuraman A, Hoogewijs D, et al. ITGA6 is directly regulated by hypoxia-inducible factors and enriches for cancer stem cell activity and invasion in metastatic breast cancer models. Mol Cancer 2016;15:26.
[28] Stewart RL, West D, Wang C, Weiss HL, Gal T, Durbin EB, et al. Elevated integrin alpha6beta4 expression is associated with venous invasion and decreased overall survival in non-small cell lung cancer. Hum Pathol 2016;54:174–83.
[29] Ammothumkandy A, Maliekal TT, Bose MV, Rajkumar T, Shirley S, Thejaswini B, et al. CD66 and CD49f expressing cells are associated with distinct neoplastic phenotypes and progression in human cervical cancer. Eur J Cancer 2016;60:166–78.
[30] Dominissini D, Moshitch-Moshkovitz S, Salmon-Divon M, Amariglio N, Rechavi G. Transcriptome-wide mapping of N(6)-methyladenosine by m(6)A-seq based on immunocapturing and massively parallel sequencing. Nat Protoc 2013;8(1):176–89.
[31] Lin S, Liu Q, Lelyveld VS, Choe J, Szostak JW, Gregory RI. Mettl1/Wdr4-mediated m(7)G tRNA Methylome is required for Normal mRNA translation and embryonic stem cell self-renewal and differentiation. Mol Cell 2018;71(2):244–55 [e245].
[32] Lin S, Choe J, Du P, Triboulet R, Gregory RI. The m(6)A methyltransferase METTL3 promotes translation in human Cancer cells. Mol Cell 2016;62(3):335–45.

[33] Liu H, Flores MA, Meng J, Zhang L, Zhao X, Rao MK, et al. MeT-DB: a database of transcriptome methylation in mammalian cells. Nucleic Acids Res 2015;43(Database issue):D197–203.
[34] Ke S, Alemu EA, Mertens C, Gantman EC, Fak JJ, Mele A, et al. A majority of m6A residues are in the last exons, allowing the potential for 3' UTR regulation. Genes Dev 2015;29(19):2037–53.
[35] Li Z, Weng H, Su R, Weng X, Zuo Z, Li C, et al. FTO plays an oncogenic role in acute myeloid leukemia as a N(6)-Methyladenosine RNA demethylase. Cancer Cell 2017;31(1):127–41.
[36] Visvanathan A, Patil V, Arora A, Hegde AS, Arivazhagan A, Santosh V, et al. Essential role of METTL3-mediated m(6)A modification in glioma stem-like cells maintenance and radioresistance. Oncogene 2018;37(4):522–33.
[37] Hynes RO. Integrins: bidirectional allosteric signaling machines. Cell 2002;110(6):673–87.
[38] Hoshino A, Costa-Silva B, Shen TL, Rodrigues G, Hashimoto A, Tesic Mark M, et al. Tumour exosome integrins determine organotropic metastasis. Nature 2015;527(7578):329–35.
[39] Stewart RL, O'Connor KL. Clinical significance of the integrin alpha6beta4 in human malignancies. Lab Inves; A J Of Tech Methods And Pathol 2015;95(9):976–86.
[40] Bigoni-Ordonez GD, Czarnowski D, Parsons T, Madlambayan GJ, Villa-Diaz LG. Integrin alpha6 (CD49f), the microenvironment and cancer stem cells. Curr Stem Cell Res Ther 2019;14(5):428–36.
[41] Hoogland AM, Verhoef EI, Roobol MJ, Schroder FH, Wildhagen MF, van der Kwast TH, et al. Validation of stem cell markers in clinical prostate cancer: alpha6-integrin is predictive for non-aggressive disease. Prostate 2014;74(5):488–96.
[42] Krebsbach PH, Villa-Diaz LG. The role of integrin alpha6 (CD49f) in stem cells: more than a conserved biomarker. Stem Cells Dev 2017;26(15):1090–9.
[43] Di Cello F, Flowers VL, Li H, Vecchio-Pagan B, Gordon B, Harbom K, et al. Cigarette smoke induces epithelial to mesenchymal transition and increases the metastatic ability of breast cancer cells. Mol Cancer 2013;12:90.
[44] Laudato S, Patil N, Abba ML, Leupold JH, Benner A, Gaiser T, et al. P53-induced miR-30e-5p inhibits colorectal cancer invasion and metastasis by targeting ITGA6 and ITGB1. Int J Cancer 2017;141(9):1879–90.
[45] Zoni E, van der Horst G, van de Merbel AF, Chen L, Rane JK, Pelger RC, et al. miR-25 modulates invasiveness and dissemination of human prostate Cancer cells via regulation of alphav- and alpha6-integrin expression. Cancer Res 2015;75(11):2326–36.
[46] Niu J, Li Z. The roles of integrin alphavbeta6 in cancer. Cancer Lett 2017;403:128–37.
[47] Behnsawy HM, Miyake H, Abdalla MA, Sayed MA, Ahmed Ael F, Fujisawa M. Expression of integrin proteins in non-muscle-invasive bladder cancer: significance of intravesical recurrence after transurethral resection. BJU Int 2011;107(2):240–6.
[48] Liu YR, Ortiz-Bonilla CJ, Lee YF. Extracellular vesicles in bladder Cancer: biomarkers and beyond. Int J Mol Sci 2018;19(9).
[49] Welton JL, Khanna S, Giles PJ, Brennan P, Brewis IA, Staffurth J, et al. Proteomics analysis of bladder cancer exosomes. Mol & Cell Proteomics : MCP 2010;9(6):1324–38.
[50] Mo Q, Nikolos F, Chen F, Tramel Z, Lee YC, Hayashi K, et al. Prognostic power of a tumor differentiation gene signature for bladder urothelial carcinomas. J Natl Cancer Inst 2018;110(5):448–59.
[51] Zhang K, Myllymaki SM, Gao P, Devarajan R, Kytola V, Nykter M, et al. Oncogenic K-Ras upregulates ITGA6 expression via FOSL1 to induce anoikis resistance and synergizes with alphaV-class integrins to promote EMT. Oncogene 2017;36(41):5681–94.
[52] Phillips JL, Taberlay PC, Woodworth AM, Hardy K, Brettingham-Moore KH, Dickinson JL, et al. Distinct mechanisms of regulation of the ITGA6 and ITGB4 genes by RUNX1 in myeloid cells. J Cell Physiol 2018;233(4):3439–53.
[53] Ying M, Tilghman J, Wei Y, Guerrero-Cazares H, Quinones-Hinojosa A, Ji H, et al. Kruppel-like factor-9 (KLF9) inhibits glioblastoma stemness through global transcription repression and integrin alpha6 inhibition. J Biol Chem 2014;289(47):32742–56.
[54] Groulx JF, Boudjadi S, Beaulieu JFMYC. Regulates alpha6 integrin subunit expression and splicing under its pro-proliferative ITGA6A form in colorectal cancer cells. Cancers 2018;10(2).
[55] Jin YP, Hu YP, Wu XS, Wu YS, Ye YY, Li HF, et al. miR-143-3p targeting of ITGA6 suppresses tumour growth and angiogenesis by downregulating PLGF expression via the PI3K/AKT pathway in gallbladder carcinoma. Cell Death Dis 2018;9(2):182.
[56] Chou J, Lin JH, Brenot A, Kim JW, Provot S, Werb Z. GATA3 suppresses metastasis and modulates the tumour microenvironment by regulating microRNA-29b expression. Nat Cell Biol 2013;15(2):201–13.
[57] Kinoshita T, Nohata N, Hanazawa T, Kikkawa N, Yamamoto N, Yoshino H, et al. Tumour-suppressive microRNA-29s inhibit cancer cell migration and invasion by targeting laminin-integrin signalling in head and neck squamous cell carcinoma. Br J Cancer 2013;109(10):2636–45.
[58] Das L, Gard JMC, Prekeris R, Nagle RB, Morrissey C, Knudsen BS, et al. Novel regulation of integrin trafficking by Rab11-FIP5 in aggressive prostate Cancer. Mol Cancer Res : MCR 2018;16(8):1319–31.
[59] Cheng M, Sheng L, Gao Q, Xiong Q, Zhang H, Wu M, et al. The m(6) Amethyltransferase METTL3 promotes bladder cancer progression via AFF4/NF-kappaB/MYC signaling network. Oncogene 2019;38(19):3667–80.
[60] Yang Y, Fan X, Mao M, Song X, Wu P, Zhang Y, et al. Extensive translation of circular RNAs driven by N(6)-methyladenosine. Cell Res 2017;27(5):626–41.